Kinetic Analysis of the Bypass of a Bulky DNA Lesion Catalyzed by Human Y-Family DNA Polymerases

ARTICLE *in* CHEMICAL RESEARCH IN TOXICOLOGY · FEBRUARY 2012

Impact Factor: 3.53 · DOI: 10.1021/tx200531y · Source: PubMed

8 AUTHORS, INCLUDING:

Laura Sanman
Stanford University
8 PUBLICATIONS **132** CITATIONS

SEE PROFILE

Chanchal Kumar Malik
Vanderbilt University
17 PUBLICATIONS **138** CITATIONS

SEE PROFILE

Ashis Basu
University of Connecticut
109 PUBLICATIONS **3,317** CITATIONS

SEE PROFILE

Published in final edited form as:
Chem Res Toxicol. 2012 March 19; 25(3): 730–740. doi:10.1021/tx200531y.

Kinetic Analysis of the Bypass of a Bulky DNA Lesion Catalyzed by Human Y-family DNA Polymerases

Shanen M. Sherrer[‡,§], **Laura E. Sanman**[‡], **Cynthia X. Xia**[‡], **Eric R. Bolin**[‡], **Chanchal K. Malik**[‖], **Georgia Efthimiopoulos**[‡], **Ashis K. Basu**[‖], and **Zucai Suo**[‡,§,*]

[‡]Department of Biochemistry, The Ohio State University, Columbus, OH 43210, USA

[§]Department of Chemistry, The Ohio State Biochemistry Program, The Ohio State University, Columbus, OH 43210, USA

[‖]Department of Chemistry, University of Connecticut, Storrs, CT 06269

Abstract

1-Nitropyrene (1-NP), a mutagen and potential carcinogen, is the most abundant nitro polyaromatic hydrocarbon in diesel exhaust, which reacts with DNA to form predominantly *N*-(deoxyguanosin-8-yl)-1-aminopyrene (dG^{AP}). If not repaired, this DNA lesion is presumably bypassed *in vivo* by any of human Y-family DNA polymerases kappa (hPolκ), iota (hPol*τ*), eta (hPol*η*), and Rev1 (hRev1). Our running start assays demonstrated that each of these enzymes was indeed capable of traversing a site-specifically placed dG^{AP} on a synthetic DNA template but hRev1 was stopped after lesion bypass. The time required to bypass 50% of the dG^{AP} sites (t_{50}^{bypass}) encountered by hPolη, hPolκ and hPolτ was determined to be 2.5 s, 4.1 s, and 106.5 s, respectively. The efficiency order of catalyzing translesion synthesis of dG^{AP} (hPolη > hPolκ > hPolτ >> hRev1) is the same as the order for these human Y-family enzymes to elongate undamaged DNA. Although hPolη bypassed dG^{AP} efficiently, replication by both hPolκ and hPolτ was strongly stalled at the lesion site and at a site immediately downstream from dG^{AP}. By employing pre-steady state kinetic methods, a kinetic basis was established for polymerase pausing at these DNA template sites. Besides efficiency of bypass, the fidelity of those low-fidelity polymerases at these pause sites was also significantly decreased. Thus, if the translesion DNA synthesis of dG^{AP} *in vivo* is catalyzed by a human Y-family DNA polymerase, *e.g.* hPolη, the process is certainly mutagenic.

INTRODUCTION

Both normal metabolic processes and environmental factors constantly damage cellular DNA and produce 1,000 to 1,000,000 DNA lesions per cell per day. If these DNA lesions are not repaired by cellular DNA repair machinery, they will stall replicative DNA polymerases and replication machinery.[1-4] To rescue stalled DNA replication, cellular DNA repair machinery temporarily switches to a Y-family DNA polymerase that primarily

*Corresponding author: Zucai Suo, 880 Biological Sciences, 484 West 12th Ave., Columbus, OH 43210; Tel: 614-688-3706; Fax: 614-292-6773; suo.3@osu.edu. .

[1]Abbreviations: AAF-dG, *N*-acetyl-2-aminofluorene adduct at the C8 position of deoxyguanosine; 1-AP, 1-aminopyrene; BPDE-dG, benzocpyrene 7,8-diol 9,10-epoxide-derived adduct at the N2 position of 2′-deoxyguanosine; BSA, bovine serum albumin; Dpo4, *Sulfolobus solfataricus* DNA polymerase IV; dG^{AP}, *N*-(deoxyguanosin-8-yl)-1-aminopyrene; dNTP, 2′-deoxynucleoside 5′-triphosphate; TLS, translesion DNA synthesis.

SUPPORTING INFORMATION AVAILABLE The structure of dG^{AP}, dG^{AP} bypass% plot, the pre-steady state kinetic parameters of each enzyme, a gel image of EMSA and corresponding plot, and the gel image displaying the efficiency of the DNA trap assay are available as supporting information. This material is available free of charge via the Internet at http://pubs.acs.org.

functions in the bypass of DNA lesions *in vivo*. Out of the 16 identified human DNA polymerases, four enzymes belong to the Y-family: DNA polymerases eta (hPolη), kappa (hPolκ), iota (hPolτ), and Rev1 (hRev1). These enzymes have been shown to catalyze both error-free and error-prone translesion DNA synthesis (TLS) *in vitro* and *in vivo*.[5-7] For example, hPolη catalyzes error-free bypass of *cis-syn* cyclobutane thymidine dimer *(cis*-syn TT)[8, 9] and its inactivation by mutations leads to Xeroderma Pigmentosum Variant (XPV) disease that increases incidence of sunlight-induced skin cancer.[8, 10] In addition, hPolη has been shown *in vitro* to bypass other lesions including apurinic/apyrimidinic (abasic) sites,[11-13] *N*-(deoxyguanosin-8-yl)-*N*-acetyl-2-aminofluorene (AAF-dG),[13] and N^2-deoxyguanosine adducts of benzo[*a*]pyrene (BPDE-dG).[12] hPolκ, a homolog of the well-studied Y-family member *Sulfolobus solfataricus* DNA Polymerase IV (Dpo4), is capable of bypassing abasic sites,[11] AAF-dG, and BPDE-dG,[14] and efficiently elongating mispaired primer termini.[15] hPolτ has been shown to bypass abasic sites,[11] *cis-syn* TT,[16] and AAF-dG.[17] hRev1 preferentially incorporates dCTP opposite any template base[18] and DNA lesions including abasic sites[11] and BPDE-dG.[19] These biochemical studies demonstrate that there is a significant overlap in lesion bypass abilities of the four human Y-family members. At present, it is unclear which human Y-family enzyme bypasses which DNA lesion(s) *in vivo*.

Despite growing concerns about the effects of air pollution on human genomic stability, there are no comprehensive studies of the bypass of air pollutant-induced DNA adducts catalyzed by human Y-family DNA polymerases. The metabolites of 1-nitropyrene (1-NP), a product of incomplete gasoline combustion and one of the most abundant polycyclic aromatic hydrocarbons (PAH),[20-22] react with DNA to primarily form *N*-(deoxyguanosin-8-yl)-1-aminopyrene (dG^{AP}, Supplementary Figure 1).[20] Because 1-NP is a potent mutagen and carcinogen in rodents,[23] it is classified as a class 2B carcinogen.[24, 25] Moreover, the dG^{AP} lesion is shown to be mutagenic in bacterial and mammalian cells.[24, 25] Thus, it is interesting to identify which human Y-family DNA polymerase(s) bypass(es) dG^{AP} *in vitro* and *in vivo*. Previously, we have shown that the kinetics of nucleotide incorporation opposite dG^{AP} and the subsequent extension of the dG^{AP} bypass product catalyzed by Dpo4 are significantly altered.[26] A minimum kinetic mechanism for the dG^{AP} bypass has also been established via pre-steady-state kinetic methods.[26] Here, we employed these methods and kinetically assessed the dG^{AP} bypass abilities of human Y-family DNA polymerases in order to shed light on which of these enzymes are better suited to bypass dG^{AP} *in vivo*.

MATERIAL AND METHODS

Materials

Reagents were purchased from the following companies: OptiKinase from USB Corporation, [γ^{-32}P]ATP from MP Biochemicals, and dNTPs from GE Healthcare. hPolη, hRev1, and hPolκ were expressed and purified as previously described.[11] hPolτ was expressed and purified as previously described[11] with one modification: the GST-tag was not removed in order to increase the protein stability of hPolτ.

DNA Substrates

The DNA template 26-mer-dG^{AP} (Table 1) was synthesized and purified as previously described.[26] Other DNA oligomers listed in Table 1 were purchased from Integrated DNA Technologies. The radiolabeling of the primers and the annealing of a primer and a template were performed as described previously.[26, 27]

Buffers

All pre-steady-state kinetic assays were performed in reaction buffer R (50 mM HEPES, pH 7.5 at 37 °C, 5 mM $MgCl_2$, 50 mM NaCl, 0.1 mM EDTA, 5 mM DTT, 10 % glycerol, and 0.1 mg/ml BSA). All electrophoresis mobility shift assays (EMSA) were performed in buffer S (50 mM Tris-Cl, pH 7.5 at 23 °C, 5 mM $MgCl_2$, 50 mM NaCl, 5 mM DTT, 10 % glycerol, and 0.1 mg/ml BSA). All reported concentrations were final after mixing solutions.

Running Start Assays

The running start assay was performed similarly as described previously.[11, 26, 28-30] Briefly, a preincubated solution of 5′-[^{32}P]-labeled DNA (100 nM) and a human Y-family enzyme (1 μM) in buffer R was rapidly mixed with a solution containing all four dNTPs (200 μM each) at 37 °C via a rapid chemical-quench flow apparatus (KinTek). The reactions were quenched with 0.37 M EDTA after various times, and the reaction products were analyzed by denaturing polyacrylamide gel electrophoresis (PAGE, 20 % polyacrylamide, 8 M urea).

Quantitative analysis of the running start assays was performed by determining the relative lesion bypass efficiencies (dG^{AP} bypass%) as a function of reaction time. For each time point *t*, dG^{AP} bypass% was calculated as the ratio of the bypass events to the encounter events (Equation 1):

$$dG^{AP}\text{bypass}\% = (B/E) \times 100\% = \{B/([20 - \text{mer}] + B)\} \times 100\% \quad (1)$$

where the total dG^{AP} bypass events (B) was calculated from the concentration of all intermediate products with sizes greater than or equal to the 21-mer, and the total dG^{AP} "encounter" events (E) equaled the summation of the 20-mer concentration and the total dG^{AP} bypass events (B). To quantitatively define the dG^{AP} bypass efficiency, t_{50}^{bypass} was defined as the time required to bypass 50% of the total dG^{AP} lesions encountered.

Electrophoresis Mobility Shift Assays

hPolη (10-400 nM), hPolκ (65-950 nM), or hRev1 (15-550 nM) was titrated onto a solution containing 5′-[^{32}P]-labeled DNA (10 nM) in buffer S at 23 °C. Native PAGE was used to separate the binary complex E•DNA from free DNA. After quantitation using a Typhoon Trio (GE Healthcare), the concentration of the binary complex was plotted as a function of the enzyme concentration. The data were fit to Equation 2 using Kaleidagraph (Synergy software):

$$[\text{E} \cdot \text{DNA}] = 0.5\left(K_{d,\text{DNA}} + \text{E}_\text{o} + \text{D}_\text{o}\right) - 0.5\left[\left(K_{d,\text{DNA}} + \text{E}_\text{o} + \text{D}_\text{o}\right)^2 - 4\text{E}_\text{o}\text{D}_\text{o}\right]^{1/2} \quad (2)$$

where E_o and D_o are the initial enzyme and DNA concentrations, respectively, and $K_{d,\text{DNA}}$ is the equilibrium dissociation constant for E•DNA at 23 °C.

Active Site Titration Assays

A preincubated solution of 5′-[^{32}P]-labeled DNA (10-450 nM) and hPolτ (27.5 nM, UV-based concentration) in buffer R was reacted with correct dNTP at saturating concentrations at 37 °C for various time intervals prior to be quenched by EDTA (0.37 M). The reaction products were resolved and quantitated as described above. The burst reaction amplitude (*A*) was plotted as a function of DNA concentrations and the data were then fit to Equation 3 to determine $K_{d,\text{DNA}}$.

$$A=0.5\left(K_{d,\mathrm{DNA}}+E_{\mathrm{o}}+\mathrm{D_o}\right)-0.5\left[\left(K_{d,\mathrm{DNA}}+\mathrm{E_o}+\mathrm{D_o}\right)^2-4\mathrm{E_oD_o}\right]^{1/2} \quad (3)$$

Nucleotide Incorporation Efficiency and Fidelity Measurements

Single-turnover kinetic assays were employed to obtain the k_p (maximum dNTP incorporation rate) and $K_{d,\ \mathrm{dNTP}}$ (equilibrium dissociation constant for dNTP from E•DNA•dNTP) for single nucleotide incorporation as described previously.[26, 31] Briefly, a preincubated solution of 5′-[^{32}P]-labeled DNA (20 nM) and hPolη (130 nM) or hPolτ (130 nM) in buffer R was mixed with increasing concentrations of an incoming dNTP at 37 °C. For hPolκ and hRev1, a preincubated solution of 5′-[^{32}P]-labeled DNA (30 nM) and hPolκ (300 nM) or hRev1 (120 nM) in buffer R was mixed with increasing concentrations of an incoming dNTP. The reactions were terminated after various times by the addition of 0.37 M EDTA. Reaction products were resolved and quantitated as described above. The time course of product formation at each dNTP concentration was fit to Equation 4:

$$[\mathrm{Product}]=A\left[1-\exp\left(-k_{\mathrm{obs}}t\right)\right] \quad (4)$$

where k_{obs} is the observed reaction rate constant. Next, the plot of the k_{obs} values as a function of dNTP concentrations was fit to Equation 5:

$$k_{\mathrm{obs}}=k_p\left[\mathrm{dNTP}\right]/\left\{\left[\mathrm{dNTP}\right]+K_{d,\mathrm{dNTP}}\right\} \quad (5)$$

From this plot, the dNTP incorporation efficiency ($k_p/K_{d,\ \mathrm{dNTP}}$) was also calculated for each enzyme. The dNTP incorporation fidelity was determined using Equation 6:

$$\mathrm{Fidelity}=\left(k_p/K_{d,\mathrm{dNTP}}\right)_{\mathrm{incorrect}}/\left[\left(k_p/K_{d,\mathrm{dNTP}}\right)_{\mathrm{correct}}+\left(k_p/K_{d,\mathrm{dNTP}}\right)_{\mathrm{incorrect}}\right] \quad (6)$$

DNA Trap Assays

A preincubated solution of hPolη (130 nM) and 5′-[^{32}P]-labeled DNA (20 nM) in buffer R was rapidly mixed with a solution of 5 μM unlabeled DNA trap D-1 (Table 1) and a correct dNTP at a saturating concentration in buffer R for various times before the reactions were quenched with 0.37 M EDTA. Reaction products were resolved and quantitated as described above. The plot of the product concentration as a function of reaction time was fit to Equation 7:

$$[\mathrm{Product}]=\mathrm{E_oA_1}\left[1-\exp\left(-k_1t\right)\right]+E_{\mathrm{o}}\mathrm{A_2}\left[1-\exp\left(-k_2\mathrm{t}\right)\right] \quad (7)$$

where $\mathrm{E_o}$ is the active hPolη concentration, $\mathrm{A_1}$ and $\mathrm{A_2}$ the reaction amplitudes of the first and second phases, respectively, and k_1 and k_2 the rate constants of the first and second phases, respectively.

RESULTS

Bypass of dG^{AP} catalyzed by human Y-family DNA polymerases

To determine if each of the four human Y-family DNA polymerases was able to bypass dG^{AP} (Supplementary Figure 1), we performed running start assays (Figure 1) with both a control DNA substrate 17-mer/26-mer and a damaged DNA substrate 17-mer/26-mer-dG^{AP} containing a site-specifically placed dG^{AP} on template 26-mer-dG^{AP} (Table 1). Notably, hPolκ synthesized much more 25-mer than 26-mer with 17-mer/26-mer after long reaction

times while an intermediate product 24-mer significantly accumulated between 6 s to 60 s (Figure 1C). Because hPolκ is known to create −1 frameshift mutations[11, 14, 32, 33] and the template 26-mer contains a dC-rich 5′-terminus (Table 1), the 25-mer was likely the true full-length product synthesized by hPolκ after hPolκ slipped once within the dC-rich region. The strong early accumulation of 24-mer in Figure 1C supports this possibility. If the possibility is proven to be true, the small amount of 26-mer was likely generated by hPolκ via a single blunt-end addition onto the 25-mer as we have previously observed with Dpo4.[34] Interestingly, the blunt-end addition phenomenon was more significant with hPolη (Figure 1A). This enzyme has been found previously to catalyze blunt-end additions onto other DNA substrates.[13, 35, 36] With the control template 26-mer, hPolη, hPolκ, and hPolτ were able to synthesize full-length products after 1 s, 6 s, and 60 s, respectively (Figures 1A, 1C, and 1E). In stark contrast, hRev1 only incorporated five nucleotides and did not synthesize full-length products even after 12 hrs (Figure 1G). The reaction was not carried out beyond 12 hrs was due to both enzyme stability and *in vivo* relevance. Interestingly, with the damaged template 26-mer-dG^{AP}, hPolη was not significantly stalled by dG^{AP} and synthesized the full-length products (26-mer and 27-mer) after 3 s (Figure 1B). In comparison, hPolκ and hPolτ needed 60 s and 7,200 s, respectively, to achieve the same task (Figures 1D and 1F). Thus, the presence of a single dG^{AP} slowed hPolκ and hPolτ by 10- and 120-fold, respectively. In addition, there was a significant accumulation of intermediate products 20-mer and 21-mer with both hPolκ and hPolτ, indicating that these enzymes encountered significant difficulty in bypassing the lesion and carrying out the subsequent extension steps (Figures 1D and 1F). As expected, hRev1, a dCTP polymerase, did not synthesize full-length products with 26-mer-dG^{AP} (Figure 1H). The longest product after 12 hrs was a small of 21-mer, suggesting that hRev1 was able to incorporate a nucleotide opposite dG^{AP} but could not extend the DNA lesion bypass product.

We further analyzed these running start assays by determining both dG^{AP} bypass% using Equation 1 (Material and Methods) and bypass efficiency t_{50}^{bypass} for each enzyme.[11] A plot of dG^{AP} bypass% versus reaction time for each enzyme (Supplementary Figure 2) yielded the corresponding t_{50}^{bypass} value (Table 2), which was defined as the time required for each enzyme to bypass 50% of the total dG^{AP} sites encountered. Similar analysis was also performed with control DNA and yielded t_{50} values for each enzyme to traverse the corresponding dG site (Table 2). These t_{50}^{bypass} values (Table 2) indicate that hPolη bypassed dG^{AP} encountered and bypassed 50% of dG^{AP} sites 1.6- and 42.6-fold faster than hPolκ and hPolτ, respectively. When comparing the t_{50}^{bypass} and t_{50} values for each enzyme, hPolη, hPolκ, and hPolτ became 3.1-, 2.7-, and 7.1-fold slower, respectively, in the presence than in the absence of dG^{AP}. Thus, dG^{AP} had only a slight inhibitory effect on the overall DNA polymerase activity of hPolη and hPolκ but significantly slowed DNA synthesis catalyzed by hPolτ. The varying effects of dG^{AP} on these three Y-family enzymes suggest that each enzyme may utilize a unique mechanism for dG^{AP} bypass.

Effects of dG^{AP} on DNA binding affinities

The accumulation of the intermediate 21-mer during dG^{AP} bypass (Figure 1) suggests that the presence of the bulky 1-AP adduct could have weakened DNA binding to human Y-family DNA polymerases. To evaluate this possibility, we estimated the binding affinity of human Y-family enzymes to 20-mer/26-mer, 20-mer/26-mer-dG^{AP}, 21-mer/26-mer, 21-mer/26-mer-dG^{AP} (Table 1) via gel electrophoresis mobility shift assays (EMSA). An example of gel image for EMSA using hPolη and 20-mer/26-mer-dG^{AP} is shown in Supplementary Figure 3. The $K_{d,\ DNA}$ values for the binding of hPolη to other DNA substrates were measured similarly and are listed in Table 3. Interestingly, the calculated ratios in Table 3 demonstrate that the presence of dG^{AP} increased the binding affinity of DNA to hPolη. The structures of Dpo4 with BPDE-dG[37] and yeast Polη with AAF-dG[38] suggest that the

hydrophobic 1-AP adduct in complexes hPolη•20-mer/26-mer-dG^{AP} and hPolη•21-mer/26-mer-dG^{AP} likely interacted with the amino acid residues in the Little Finger domain of hPolη.

When EMSA was performed for each of the other human Y-family enzymes, we were only able to estimate the $K_{d,\ DNA}$ values for hRev1 (Table 3). There was no obvious mobility shift with hPolκ and hPolτ during EMSA, likely due to their weak binding to DNA. For hPolτ, active site titration assays (Materials and Methods) were employed to estimate the $K_{d,\ DNA}$ values (Table 3). These values were similar to a previously reported value of 44 ± 7 nM with an undamaged DNA substrate.[39] We did not measure the $K_{d,\ DNA}$ of hPolτ•21-mer/26-mer-dG^{AP} because catalysis (see below) was slower than the equilibration of the enzyme and DNA (E + DNA ↔ E•DNA). For hPolκ, it is not proper to use active site titration assays to estimate the $K_{d,\ DNA}$ values because only 15% of recombinant hPolκ has been previously found to be active in such an assay.[40] With undamaged DNA, the $K_{d,\ DNA}$ of a similar hPolκ construct used in this paper (Materials and Methods) has been estimated to be 96 ± 21 nM at 25 °C by using a fluorescence anisotropy assay.[41] Based on the above published and measured $K_{d,\ DNA}$ values as well as calculated affinity ratios in Table 3, we concluded that hPolη bound to both damaged and undamaged DNA with the highest affinity and the impact of the 1-AP adduct on DNA binding to human Y-family DNA polymerases was not significant enough to account for the strong polymerase pausing during TLS shown in Figure 1. As we have discovered previously with other DNA lesions,[26, 29, 42] it is likely that nucleotide incorporation kinetics was dramatically influenced by dG^{AP}.

Effect of dG^{AP} on the kinetics of nucleotide incorporation

hPolη—To determine the effect of dG^{AP} on nucleotide incorporation efficiency at or near the lesion site, we performed single nucleotide incorporation assays with each human Y-family DNA polymerase under single-turnover conditions. For example, a preincubated solution of 5′-[^{32}P]-labeled DNA 20-mer/26-mer-dG^{AP} (20 nM) and hPolη (130 nM) at 37 °C was rapidly mixed with varying dCTP concentrations for various reaction times before being quenched with EDTA (0.37 M). The reaction mixtures were analyzed by denaturing PAGE and quantitated by using a Typhoon Trio (Materials and Methods). Subsequently, the product concentrations were plotted against reaction times and each time course was fit to Equation 4 to obtain an observed reaction rate constant (k_{obs}) (Figure 2A). The plot of the k_{obs} values versus dCTP concentrations was then fit to Equation 5 to obtain an apparent maximum dCTP incorporation rate constant (k_p) of 8.1 ± 0.2 s^{-1} and an apparent equilibrium dissociation constant ($K_{d,\ dNTP}$) of 287 ± 24 μM opposite dG^{AP} (Figure 2B). The efficiency ($k_p/K_{d,\ dNTP}$) of correct dCTP incorporation opposite dG^{AP} was then calculated to be 2.8×10^{-2} $\mu M^{-1}s^{-1}$ (Table 4).

To determine if nucleotide incorporation efficiency and fidelity were affected within the vicinity of the bulky 1-AP adduct, we performed similar single-turnover kinetic assays for each correct or incorrect nucleotide with control or damaged DNA substrates and the resulting kinetic parameters are listed in Table 4 and Supplementary Table 1. In the presence of either 20-mer/26-mer or 21-mer/26-mer (Table 1), hPolη incorporated correct nucleotides with 50-500 fold higher $k_p/K_{d,\ dNTP}$ values than incorrect nucleotides, which are mainly derived from the k_p differences (Supplementary Table 1). Relative to corresponding control DNA substrates, hPolη incorporated correct nucleotides onto 20-mer/26-mer-dG^{AP} and 21-mer/26-mer-dG^{AP} with 6-18 fold lower k_p values and 3-fold higher $K_{d,\ dNTP}$ values, leading to 20-48 fold lower $k_p/K_{d,\ dNTP}$ values (Table 4). The large decreases in nucleotide incorporation efficiency with the damaged DNA appear to be contradictory to the conclusion of weak polymerase pausing as revealed by Figure 1B. However, the overall polymerase efficiency at the lesion site and the immediate downstream site only dropped by

7-16 fold if the 3-fold tighter DNA binding affinity (Table 3) was taken into consideration. Moreover, the relative high k_p values (2-8 s^{-1}) for correct nucleotide incorporation further diminished intermediate product accumulation near the lesion site in Figure 1B. Interestingly, the nucleotide incorporation fidelity of hPolη was 16-fold lower on average with the damaged DNA substrates than undamaged ones and thus, significant percentages of incorporated nucleotides opposite dG^{AP} and the downstream template base dC were incorrect (Table 4). Remarkably, hPolη misincorporated dCTP onto 21-mer/26-mer-dG^{AP} with 3-fold higher k_p and $k_p/K_{d,\ dNTP}$ values than it incorporated correct dGTP. Taken together, hPolη was highly error-prone although it catalyzed efficient TLS of dG^{AP}.

hPolκ—The kinetic parameters for correct and incorrect nucleotide incorporations with control (Supplementary Table 2) and damaged (Table 5) DNA substrates were determined under similar single-turnover kinetic conditions as described for hPolη (Supplementary Figure 4). Like hPolη, hPolκ incorporated correct dNTPs onto damaged DNA with decreased efficiency than onto undamaged DNA. Notably, the decrease is less dramatic during the dG^{AP} bypass step (5.7-fold) than during the extension step (208-fold) and hPolκ was 123-fold less efficient during the later step than during the former step. These efficiency differences and the low k_p value (2.3×10^{-3} s^{-1}) for correct dGTP incorporation onto 21-mer/26-mer-dG^{AP} contributed to the strong accumulation of the intermediate product 21-mer (Figure 1D).

With control DNA substrates, the nucleotide incorporation fidelity of hPolκ was calculated to be in the range of 10^{-3} to 10^{-2} (Supplementary Table 2). The low nucleotide incorporation fidelity of hPolκ was further worsened by 2-94 folds and was in the range of 10^{-2} to 10^{-1} with the damaged DNA substrates (Table 5). The probability for hPolκ to incorporate incorrect nucleotides during TLS of dG^{AP} was estimated to be as high as 30% (Table 5).

hPolτ—Like hPolη and hPolκ, the kinetic parameters for nucleotide incorporations with undamaged (Supplementary Table 3) and damaged (Table 6) DNA substrates were determined by employing single-turnover kinetic assays (Supplementary Figure 5). Since misincorporation of either dATP or dCTP onto 21-mer/26-mer-dG^{AP} catalyzed by hPolτ was not detected even after eight hours, the corresponding kinetic parameters with either 21-mer/26-mer-dG^{AP} or 21-mer/26-mer were not determined. Like hPolκ, hPolτ incorporated correct nucleotides onto damaged DNA with lower efficiency than onto undamaged DNA and the impact was determined to be 7- and 4,545-fold with 20-mer/26-mer-dG^{AP} and 21-mer/26-mer-dG^{AP}, respectively (Table 6). Accordingly, 21-mer/26-mer-dG^{AP} was extended by hPolτ with more than 1,000-fold lower k_p and $k_p/K_{d,\ dNTP}$ values than 20-mer/26-mer-dG^{AP}. These kinetic differences led to the strong accumulation of the intermediate product 21-mer in Figure 1F.

With 20-mer/26-mer-dG^{AP}, all three incorrect nucleotides were incorporated onto 20-mer/26-mer-dG^{AP} by hPolτ with comparable low efficiencies and probabilities (Table 6). In comparison, incorrect dTTP was incorporated onto 21-mer/26-mer-dG^{AP} with similar efficiency and probability to those of correct dGTP (Table 6). These kinetic data suggest that hPolτ was more error-prone during the subsequent extension step than during dG^{AP} bypass.

hRev1—Consistent with Figure 1H, hRev1 could not incorporate any nucleotide onto 21-mer/26-mer-dG^{AP} after three hours. Thus, we only determined the kinetic parameters for nucleotide incorporations onto 20-mer/26-mer-dG^{AP} (Table 7) and the corresponding control substrate 20-mer/26-mer (Supplementary Table 4) under single turnover conditions (Supplementary Figure 6). Like the other three human Y-family enzymes, hRev1 incorporated dCTP opposite dG^{AP} with 22-fold lower efficiency than opposite undamaged

dG, which was predominantly contributed by the k_p difference. In addition, all three incorrect dNTPs were also incorporated with lower efficiency when the template base dG was damaged, leading to a higher fidelity with 20-mer/26-mer-dG^{AP}. Thus, hRev1 was slightly more error-free but catalytically slower as it bypassed dG^{AP}.

Biphasic kinetics of nucleotide incorporation catalyzed by hPolη

Previously, we have shown that correct nucleotide incorporation opposite dG^{AP} and the downstream template base dC catalyzed by Dpo4 in the presence of a DNA trap follows biphasic kinetics and that the amplitudes of both the fast and slow phases are higher during the dG^{AP} bypass step.[26] To explore if human Y-family DNA polymerases also follow similar biphasic kinetics during dG^{AP} bypass in the presence of a DNA trap, hPolη was chosen as a model enzyme because it bound DNA tightly (Table 3), a condition for the DNA trap assay.[26, 29, 42-45] Here, we performed single dGTP incorporation onto either 21-mer/26-mer or 21-mer/26-mer-dG^{AP} in the presence of an unlabeled DNA trap which was in large excess over 5′-radiolabeled DNA. First, we determined the effectiveness of 5 μM D-1 (Table 1) as a DNA trap. This trap was effective to prevent correct dGTP incorporation onto radiolabeled 21-mer/26-mer (20 nM) by hPolη within 33 s (Supplementary Figure 7). Next, we conducted the DNA trap assay for correct dGTP incorporation onto either 21-mer/26-mer or 21-mer/26-mer-dG^{AP} (Material and Methods). The concentration of products was plotted as a function of reaction time (Figure 3) and the plot was fit to Equation 6 to yield kinetic parameters listed in Supplementary Table 5. Unlike Dpo4,[26] hPolη followed biphasic kinetics with both control and damaged DNA substrates. With 21-mer/26-mer, the amplitude of the fast kinetic phase (A_1 = 39%) is smaller than that of the slow kinetic phase (A_2 = 47%) while the former (k_1 = 72.2 s^{-1}) occurs with a higher reaction rate constant than the latter (k_2 = 4.4 s^{-1}). Interestingly, the sum of the fast and slow reaction rate constants ($A_1k_1 + A_2k_2$ = 30 s^{-1}) for 21-mer/26-mer is close to the k_p value (39 s^{-1}, Supplementary Table 1) determined by using the single-turnover kinetic assay. For dGTP incorporation onto 21-mer/26-mer-dG^{AP}, both A_1 and k_1 were larger than corresponding A_2 and k_2 (Supplementary Table 5). The sum of reaction rate constants for 21-mer/26-mer-dG^{AP} ($A_1k_1 + A_2k_2$ = 1.5 s^{-1}) is also approximately equal to the k_p value in Table 4 (2.2 s^{-1}). Similar relationship has been previously observed with other lesions and Dpo4.[26, 29, 42-45] This is not surprising because both k_p and the sum ($A_1k_1 + A_2k_2$) reflect the rate constant of nucleotide incorporation during single binding event between an enzyme and DNA. Furthermore, all four biphasic kinetic parameters with 21-mer/26-mer-dG^{AP} are smaller than the counterparts with 21-mer/26-mer, suggesting that the presence of dG^{AP} negatively affected the biphasic kinetics of nucleotide incorporation in the presence of a DNA trap.

DISCUSSION

In this paper, we have compared the abilities of four human Y-family DNA polymerases to catalyze TLS of dG^{AP} in the same reaction conditions. All of them except hRev1 bypassed a single site-specifically placed lesion dG^{AP} and synthesized full-length products with different efficiency (Figure 1, Table 2). There was more accumulation of the intermediate product 21-mer than 20-mer synthesized by hPolκ (Figure 1D) and hPolτ (Figure 1F). This suggests that for these enzymes, the dG^{AP} bypass step was less problematic than the subsequent extension step. Similar strong polymerase pausing immediately downstream from a bulky DNA lesion site has also been observed for the bypass of dG^{AP} [26] and AAF-dG[46] catalyzed by Dpo4 and for the bypass of BPDE-dG[47] and AAF-dG catalyzed by yeast Polη.[38] To understand the polymerization patterns in Figure 1, it is necessary to establish a kinetic basis for how each human Y-family DNA polymerase catalyzes TLS of dG^{AP}.

Comparison of efficiency of human Y-family DNA polymerases with undamaged DNA

For efficient DNA synthesis, a DNA polymerase must bind to DNA tightly and incorporate nucleotides with high substrate specificity ($k_p/K_{d,\ dNTP}$). Since the $K_{d,\ DNA}$ values do not change significantly within the temperature range of 23 to 37 °C, we ranked the DNA-binding affinity order of human Y-family enzymes as hPolη > hPolτ > hPolκ ≈ hRev1 based on the $K_{d,\ DNA}$ values (Table 3) and the affinity of undamaged DNA to hPolκ (96 ± 21 nM) measured by fluorescence anisotropy at 25 °C.[41] Notably, the $K_{d,\ DNA}$ values of human Y-family DNA polymerases were within 5-fold and are not the major factor to differentiate their relative polymerization efficiency. In contrast, the $k_p/K_{d,\ dNTP}$ values for correct nucleotide incorporation onto undamaged DNA by these enzymes varied by several orders of magnitude (Supplementary Tables 1-4) and likely governed the polymerization efficiency order. For example, the order of $k_p/K_{d,\ dNTP}$ values of dCTP incorporation opposite dG in 20-mer/26-mer was as followed: hPolη (0.56 $\mu M^{-1}s^{-1}$) > hRev1 (0.14 $\mu M^{-1}s^{-1}$) > hPolκ (0.037 $\mu M^{-1}s^{-1}$) > hPolτ (0.0016 $\mu M^{-1}s^{-1}$). Similarly, the $k_p/K_{d,\ dGTP}$ values for correct dGTP incorporation onto 21-mer/26-mer were ranked as hPolη (0.84 $\mu M^{-1}s^{-1}$) > hPolκ (0.011 $\mu M^{-1}s^{-1}$) > hPolτ (0.0016 $\mu M^{-1}s^{-1}$). Although we did not measure the $k_p/K_{d,\ dNTP}$ value for dGTP incorporation onto 21-mer/26-mer by hRev1, our previous work has shown that this deoxycytidyl transferase preferentially incorporates dCTP, rather than a correct incoming nucleotide, opposite dC, dA, or dT with 10^3-10^4 fold lower $k_p/K_{d,\ dNTP}$ than incorporating dCTP opposite dG.[18] Accordingly, the $k_p/K_{d,\ dNTP}$ values for dGTP incorporation onto 21-mer/26-mer follow the order of hPolη > hPolκ > hPolτ > hRev1. Although we did not determine the $k_p/K_{d,\ dNTP}$ values for correct dNTP incorporations at other positions along template 26-mer, the $k_p/K_{d,\ dNTP}$ order was expected to follow hPolη > hRev1 > hPolκ > hPolτ at each of the two template dG positions and hPolη > hPolκ > hPolτ > hRev1 at each of the other five template positions. Taken together, the overall efficiency for the elongation of primer 17-mer to 26-mer along the template 26-mer is expected to follow the order of hPolη > hPolκ > hPolτ >> hRev1. Interestingly, this prediction was consistent with the speed order of elongating 17-mer/26-mer to full-length products by human Y-family enzymes: hPolη (1 s) > hPolκ (6 s) > hPolτ (60 s) >> hRev1 (> 12 hrs) (Figure 1).

Comparison of the TLS of dG^{AP} efficiency catalyzed by human Y-family DNA polymerases

When human Y-family enzymes elongated 17-mer along 26-mer-dG^{AP} (Figure 1) the most troubled steps were the dG^{AP} bypass step and the subsequent extension step. Opposite dG^{AP}, dCTP was incorporated onto 20-mer/26-mer-dG^{AP} with the following efficiency order of hPolη (2.8×10^{-2} $\mu M^{-1}s^{-1}$) > hRev1 = hPolκ (6.5×10^{-3} $\mu M^{-1}s^{-1}$) > hPolτ (2.3×10^{-4} $\mu M^{-1}s^{-1}$) (Tables 4-6), which is consistent with the t_{50}^{bypass} order of hPolη (2.5 s) < hPolκ (4.1 s) < hPolτ (107 s) (Table 2). During the subsequent extension step, dGTP was incorporated opposite dC in 21-mer/26-mer-dG^{AP} with the $k_p/K_{d,\ dNTP}$ order of hPolη (1.8×10^{-2} $\mu M^{-1}s^{-1}$ > hPolκ (5.3×10^{-5} $\mu M^{-1}s^{-1}$) > hPolτ (2.2×10^{-7} $\mu M^{-1}s^{-1}$). Since hRev1 did not elongate 21-mer/26-mer-dG^{AP} after several hours, its $k_p/K_{d,\ dNTP}$ value should be much lower than that of hPolτ. Thus, the order of nucleotide incorporation efficiency during the extension step is hPolη > hPolκ > hPolτ >> hRev1. On the basis of these $k_p/K_{d,\ dNTP}$ values and the small impact of dG^{AP} on the $K_{d,\ DNA}$ values (Results), we predicted that the overall efficiency of TLS of dG^{AP} and possibly the elongation of 17-mer/26-mer-dG^{AP} to full-length products follow the order of hPolη > hPolκ > hPolτ >> hRev1. Consistently, this order matched the speed order for creating full-length product 26-mer along template 26-mer-dG^{AP} (Figure 1). Thus, hPolη is the most efficient human Y-family DNA polymerase to catalyze TLS of dG^{AP}. Interestingly, the same conclusion has been reached by us for the TLS of an abasic site.[11]

A kinetic basis for polymerase pausing during TLS of dG^{AP}

In the presence of dG^{AP}, the accumulation of the intermediate products 20-mer and 21-mer was more obvious with hPolκ (Figure 1D) and hPolτ (Figure 1F) than with hPolη (Figure 1B). These data indicated that these former enzymes had different extents of difficulty in either binding damaged DNA or incorporating nucleotides opposite both dG^{AP} and the downstream template base dC on template 26-mer-dG^{AP}. Table 3 displays the small impact of dG^{AP} on the $K_{d,\ DNA}$ values of human Y-family DNA polymerases. In contrast, the $k_p/K_{d,\ dNTP}$ values were drastically affected by the presence of dG^{AP} (Tables 4-6). For example, hPolη, hPolκ, and hPolτ were 20-, 6-, and 208-fold, respectively, less efficient when incorporating dCTP opposite dG^{AP} than opposite dG in undamaged DNA. During the subsequent extension step, the embedded dG^{AP} affected the $k_p/K_{d,\ dNTP}$ values of hPolη, hPolκ, and hPolτ by 48-, 208-, and 4,565-fold, respectively. Thus, the large decrease in correct nucleotide incorporation efficiency caused by dG^{AP} was the main reason why these human Y-family enzymes paused during TLS of dG^{AP} (Figure 1). Specifically, the decreases in $k_p/K_{d,\ dNTP}$ values were contributed by 2-4 fold higher $K_{d,\ dNTP}$ values and up to 1,000-fold lower k_p values. In addition, the larger negative effect of dG^{AP} on the $k_p/K_{d,\ dNTP}$ values of hPolκ and hPolτ than on those of hPolη explained why both hPolκ and hPolτ paused more strongly than hPolη at the 20th and 21st template positions (Figure 1). The 3-fold higher binding affinity of hPolη to damaged DNA than to undamaged DNA (Table 3) and relatively high k_p values (2 to 8 s^{-1}) for correct nucleotide incorporations opposite both dG^{AP} and downstream dC (Table 4) further lessened hPolη pausing at these sites.

Clearly, the intermediate product 21-mer accumulated more than 20-mer with both hPolκ (Figure 1D) and hPolτ (Figure 1F). This observation suggested that the subsequent extension step was affected by dG^{AP} more than the DNA lesion bypass step with these enzymes. Consistently, the $k_p/K_{d,\ dNTP}$ value for correct nucleotide incorporation was 123-fold lower during the extension step than during the lesion bypass step with hPolκ (Table 5) while the difference was 1,045-fold lower with hPolτ (Table 6). Additionally, these efficiency differences were mainly contributed by ~1,000-fold decrease in k_p. Thus, the conversion from 21-mer to 22-mer was less efficient and much slower than the conversion from 20-mer to 21-mer, leading to the stronger accumulation of 21-mer in Figures 1D and 1F.

Biphasic kinetics of nucleotide incorporation with hPolη

Surprisingly, we observed a fast phase (A_1 = 39%, k_1 = 72.2 s^{-1}) and a slow phase (A_2 = 47%, k_2 = 4.4 s^{-1}) during correct nucleotide incorporation onto undamaged 21-mer/26-mer catalyzed by hPolη in the presence of a DNA trap (Figure 3). In contrast, only the fast phase has been observed during nucleotide incorporation onto the same undamaged substrate catalyzed by Dpo4.[26] At present, it is unclear what contributed to the slow phase observed with hPolη. Mechanistically, it is possible that 39% of the binary complex hPolη•DNA were in a productive conformation (E•DNA$_n^P$) while 47% of the complex were in a slightly non-productive manner (E•DNA$_n^N$). The latter was isomerized to become the former at a rate of 4.4 s^{-1}. Since the total reaction amplitude (A_1 + A_2) of 86% is close to the calculated percentage of the binary complex (83%) based on the $K_{d,\ DNA}$ value (Table 3), the remaining 14% of 21-mer/26-mer must not be bound by hPolη and were free in solution. For the unprecedented biphasic kinetics of nucleotide incorporation onto normal DNA, we proposed a mechanism shown in Figure 4A.

Like Dpo4,[26] biphasic kinetics of correct dNTP incorporation onto 21-mer/26-mer-dG^{AP} was observed with hPolη (Figure 3). In comparison to what was observed with 21-mer/26-mer, the total reaction amplitude of the fast (14%) and slow (5.3%) phases with 21-mer/26-mer-dG^{AP} was only 19.3%, much less than the calculated reaction amplitude (93%) based

on the $K_{d,\ DNA}$ value in Table 3. Besides the decrease in reaction amplitudes in both phases, the values of k_1 and k_2 were also reduced by the presence of the bulky 1-AP adduct (Supplementary Table 5). Based on the above calculation, 7% of 21-mer/26-mer-dG^{AP} was free in solution and 73.7% were in a dead-end conformation (E•DNA$_n^D$) which was not elongated within the observation time window in Figure 3. The physical nature of E•DNA$_n^D$ is unclear at present. It is likely that hPolη bound to DNA in a catalytically incompetent conformation. It is also possible that some hPolη molecules bound to the blunt-end of 21-mer/26-mer-dG^{AP}, rather than the staggered end, as suggested by the formation of 27-mer through a blunt-end addition (Figure 1B). On the basis of the above information, we proposed a kinetic mechanism for TLS of dG^{AP} shown in Figure 4B, which has been previously applied to other DNA lesions and polymerases.[26, 29, 42, 44] There are a few indirect structural evidences to support this mechanism. Previously, the NMR structure of a damaged 11-mer duplex reveals that the hydrophobic 1-AP adduct of an embedded dG^{AP}:dC base pair is intercalated onto the DNA helix between adjacent Watson-Crick base pairs with the sugar of the modified dG possessing a *syn* glycosidic torsion angle, and the bases of the dG^{AP}:dC base pair are displaced onto the major groove.[48] If this conformation of dG^{AP} is preserved within the active site of hPolη, the bulky 1-AP adduct would occupy the position of an incoming dNTP. Such a binary complex would not be elongated without undergoing dramatic structural changes and likely represents E•DNA$_n^D$. Consistently, a crystal structure of the binary complex of yeast Polη and DNA containing an AAF-dG[38] shows that the AAF adduct stacks above the last primer-template base pair as proposed for E•DNA$_n^D$. The other crystal structure of the same binary complex illustrates that the enzyme rotates along DNA and allows the DNA adduct to partially block the active site. If 1-AP is in the quasi-intercalative conformation as AAF in the corresponding binary crystal structure, the binary complex hPolη•20-mer/26-mer-dG^{AP} requires subtle to mild structural changes before elongation and thereby exists in the conformation of E•DNA$_n^N$. When 1-AP is completely rotated out of the DNA duplex, hPolη•21-mer/26-mer-dG^{AP} will be in the conformation of E•DNA$_n^P$ and be rapidly elongated after nucleotide binding.

Impact of dG^{AP} on polymerase fidelity

The fidelity of nucleotide incorporation opposite dG^{AP} (Tables 4-7) ranked as hRev1 (10^{-4}) > hPolτ (10^{-3} to 10^{-2}) > hPolη (10^{-2} to 10^{-1}) = hPolκ (10^{-2} to 10^{-1}). The calculated fidelity ratios implied that both hPolη and hPolκ were about 10-fold more error-prone when opposite dG^{AP} than opposite undamaged dG. Interestingly, the bulky 1-AP adduct enhanced the fidelity of hRev1 significantly and hPolτ slightly during dG^{AP} bypass. Such an impact of the 1-AP adduct on polymerase fidelity was more negatively significant during the subsequent extension step. Opposite 5′-dC from dG^{AP}, hPolη incorporated incorrect dCTP with 3-fold higher efficiency than correct dGTP, hPolκ incorporated incorrect dATP with only 2-fold lower efficiency than correct dGTP, and hPolτ incorporated both correct dGTP and incorrect dTTP with almost equal $k_p/K_{d,\ dNTP}$ values, leading to lowered polymerase fidelity at this position (Tables 4-6). Taken together, our kinetic studies suggested that hPolη, hPolκ and hPolτ became more error-prone during TLS of dG^{AP} than during normal DNA synthesis.

The pathways for the formation of DNA lesions *in vivo* and whether the DNA lesions stall cellular DNA replication machinery have not been thoroughly explored.[49] So far, it is known that genetic markers, *e.g. Umu* gene, for mutagenesis activity in several cell lines are elevated in the presence of 1-NP or certain metabolites.[21-25] These results suggest that the Y-family DNA polymerases are active in the presence of lesion dG^{AP}. If so, the mutagenic bypass of dG^{AP} catalyzed by these enzymes may lead to genetic mutations *in vivo*.[25, 50-54]

In summary, our kinetic data demonstrated that hPolη, hPolκ, and hPolτ were able to bypass dG^{AP} and extend the lesion bypass product with dramatically different efficiency and

fidelity values. In contrast, hRev1 was only able to bypass the bulky DNA lesion. A kinetic basis for polymerase pausing during error-prone TLS of dG^{AP} was established.

Supplementary Material

Refer to Web version on PubMed Central for supplementary material.

Acknowledgments

We sincerely thank David Beyer, Jessica Chadwick and Rebecca Frankel for their assistance in performing some of the single-turnover kinetic assays with hRev1 and hPolκ. We also thank Jason Fowler and Sean Newmister for purifying hRev1 and hPolκ.

FUNDING SUPPORT

This work was supported by National Science Foundation Career Award (MCB-0447899) to Z.S., National Science Foundation Grant (MCB-0960961) to Z.S., and National Institutes of Health Grant (ES009127) to A.K.B. and Z.S. S.M.S was supported by an American Heart Association Predoctoral Fellowship (Grant GRT00014861).

REFERENCES

(1). Duvauchelle JB, Blanco L, Fuchs RP, Cordonnier AM. Human DNA polymerase mu (Pol mu) exhibits an unusual replication slippage ability at AAF lesion. Nucleic Acids Res. 2002; 30:2061–2067. [PubMed: 11972346]

(2). Kunkel TA. DNA replication fidelity. J. Biol. Chem. 2004; 279:16895–16898. [PubMed: 14988392]

(3). Freisinger E, Grollman AP, Miller H, Kisker C. Lesion (in)tolerance reveals insights into DNA replication fidelity. Embo J. 2004; 23:1494–1505. [PubMed: 15057282]

(4). Gruz P, Shimizu M, Pisani FM, De Felice M, Kanke Y, Nohmi T. Processing of DNA lesions by archaeal DNA polymerases from Sulfolobus solfataricus. Nucleic Acids Res. 2003; 31:4024–4030. [PubMed: 12853619]

(5). Boudsocq F, Ling H, Yang W, Woodgate R. Structure-based interpretation of missense mutations in Y-family DNA polymerases and their implications for polymerase function and lesion bypass. DNA Repair (Amst). 2002; 1:343–358. [PubMed: 12509239]

(6). Goodman MF. Error-prone repair DNA polymerases in prokaryotes and eukaryotes. Annu. Rev. Biochem. 2002; 71:17–50. [PubMed: 12045089]

(7). Lehmann AR. Replication of damaged DNA in mammalian cells: new solutions to an old problem. Mutat. Res. 2002; 509:23–34. [PubMed: 12427529]

(8). Masutani C, Kusumoto R, Yamada A, Dohmae N, Yokoi M, Yuasa M, Araki M, Iwai S, Takio K, Hanaoka F. The XPV (xeroderma pigmentosum variant) gene encodes human DNA polymerase eta. Nature. 1999; 399:700–704. [PubMed: 10385124]

(9). Masutani C, Araki M, Yamada A, Kusumoto R, Nogimori T, Maekawa T, Iwai S, Hanaoka F. Xeroderma pigmentosum variant (XP-V) correcting protein from HeLa cells has a thymine dimer bypass DNA polymerase activity. EMBO J. 1999; 18:3491–3501. [PubMed: 10369688]

(10). Johnson RE, Kondratick CM, Prakash S, Prakash L. hRAD30 mutations in the variant form of xeroderma pigmentosum. Science. 1999; 285:263–265. [PubMed: 10398605]

(11). Sherrer SM, Fiala KA, Fowler JD, Newmister SA, Pryor JM, Suo Z. Quantitative analysis of the efficiency and mutagenic spectra of abasic lesion bypass catalyzed by human Y-family DNA polymerases. Nucleic Acids Res. 2011; 39:609–622. [PubMed: 20846959]

(12). Zhang Y, Yuan F, Wu X, Rechkoblit O, Taylor JS, Geacintov NE, Wang Z. Error-prone lesion bypass by human DNA polymerase eta. Nucleic Acids Res. 2000; 28:4717–4724. [PubMed: 11095682]

(13). Masutani C, Kusumoto R, Iwai S, Hanaoka F. Mechanisms of accurate translesion synthesis by human polymerase eta. Embo J. 2000; 19:3100–3109. [PubMed: 10856253]

(14). Zhang Y, Yuan F, Xin H, Wu X, Rajpal DK, Yang D, Wang Z. Human DNA polymerase kappa synthesizes DNA with extraordinarily low fidelity. Nucleic Acids Res. 2000; 28:4147–4156. [PubMed: 11058111]

(15). Washington MT, Johnson RE, Prakash L, Prakash S. Human DINB1-encoded DNA polymerase kappa is a promiscuous extender of mispaired primer termini. Proc. Natl. Acad. Sci. U. S. A. 2002; 99:1910–1914. [PubMed: 11842189]

(16). Haracska L, Johnson RE, Unk I, Phillips BB, Hurwitz J, Prakash L, Prakash S. Targeting of human DNA polymerase iota to the replication machinery via interaction with PCNA. Proc. Natl. Acad. Sci. U. S. A. 2001; 98:14256–14261. [PubMed: 11724965]

(17). Zhang Y, Yuan F, Wu X, Taylor JS, Wang Z. Response of human DNA polymerase iota to DNA lesions. Nucleic Acids Res. 2001; 29:928–935. [PubMed: 11160925]

(18). Brown JA, Fowler JD, Suo Z. Kinetic basis of nucleotide selection employed by a protein template-dependent DNA polymerase. Biochemistry. 2010; 49:5504–5510. [PubMed: 20518555]

(19). Zhang Y, Wu X, Rechkoblit O, Geacintov NE, Taylor JS, Wang Z. Response of human REV1 to different DNA damage: preferential dCMP insertion opposite the lesion. Nucleic Acids Res. 2002; 30:1630–1638. [PubMed: 11917024]

(20). Mitchelmore CL, Livingstone DR, Chipman JK. Conversion of 1-nitropyrene by Brown trout (Salmo trutta) and turbot (Scophtalamus maximus) to DNA adducts detected by 32P-postlabelling. Biomarkers. 1998; 3:21–33.

(21). Pohjola SK, Lappi M, Honkanen M, Rantanen L, Savela K. DNA binding of polycyclic aromatic hydrocarbons in a human bronchial epithelial cell line treated with diesel and gasoline particulate extracts and benzo[a]pyrene. Mutagenesis. 2003; 18:429–438. [PubMed: 12960411]

(22). Pohjola SK, Savela K, Kuusimaki L, Kanno T, Kawanishi M, Weyand E. Polycyclic aromatic hydrocarbons of diesel and gasoline exhaust and DNA adduct detection in calf thymus DNA and lymphocyte DNA of workers exposed to diesel exhaust. Polycyclic Aromatic Compounds. 2004; 24:451–465.

(23). Hirose M, Lee MS, Wang CY, King CM. Induction of rat mammary gland tumors by 1-nitropyrene, a recently recognized environmental mutagen. Cancer Res. 1984; 44:1158–1162. [PubMed: 6692400]

(24). Sabbioni G, Jones CR. Biomonitoring of arylamines and nitroarenes. Biomarkers. 2002; 7:347–421. [PubMed: 12437855]

(25). Malia SA, Vyas RR, Basu AK. Site-specific frame-shift mutagenesis by the 1-nitropyrene-DNA adduct N-(deoxyguanosin-8-y1)-1-aminopyrene located in the (CG)3 sequence: effects of SOS, proofreading, and mismatch repair. Biochemistry. 1996; 35:4568–4577. [PubMed: 8605207]

(26). Sherrer SM, Brown JA, Pack LR, Jasti VP, Fowler JD, Basu AK, Suo Z. Mechanistic studies of the bypass of a bulky single-base lesion catalyzed by a Y-family DNA polymerase. J. Biol. Chem. 2009; 284:6379–6388. [PubMed: 19124465]

(27). Zhang L, Brown JA, Newmister SA, Suo Z. Polymerization fidelity of a replicative DNA polymerase from the hyperthermophilic archaeon Sulfolobus solfataricus P2. Biochemistry. 2009; 48:7492–7501. [PubMed: 19456141]

(28). Fiala KA, Suo Z. Sloppy bypass of an abasic lesion catalyzed by a Y-family DNA polymerase. J. Biol. Chem. 2007; 282:8199–8206. [PubMed: 17234630]

(29). Brown JA, Newmister SA, Fiala KA, Suo Z. Mechanism of double-base lesion bypass catalyzed by a Y-family DNA polymerase. Nucleic Acids Res. 2008; 36:3867–3878. [PubMed: 18499711]

(30). Brown JA, Pack LR, Fowler JD, Suo Z. Pre-steady-state kinetic analysis of the incorporation of anti-HIV nucleotide analogs catalyzed by human X- and Y-family DNA polymerases. Antimicrob. Agents Chemother. 2011; 55:276–283. [PubMed: 21078938]

(31). Fiala KA, Suo Z. Pre-Steady-State Kinetic Studies of the Fidelity of Sulfolobus solfataricus P2 DNA Polymerase IV. Biochemistry. 2004; 43:2106–2115. [PubMed: 14967050]

(32). Yang W, Woodgate R. What a difference a decade makes: insights into translesion DNA synthesis. Proc. Natl. Acad. Sci. U. S. A. 2007; 104:15591–15598. [PubMed: 17898175]

(33). Choi JY, Chowdhury G, Zang H, Angel KC, Vu CC, Peterson LA, Guengerich FP. Translesion synthesis across O6-alkylguanine DNA adducts by recombinant human DNA polymerases. J. Biol. Chem. 2006; 281:38244–38256. [PubMed: 17050527]

(34). Fiala KA, Brown JA, Ling H, Kshetry AK, Zhang J, Taylor JS, Yang W, Suo Z. Mechanism of template-independent nucleotide incorporation catalyzed by a template-dependent DNA polymerase. J. Mol. Biol. 2007; 365:590–602. [PubMed: 17095011]

(35). McCulloch SD, Kokoska RJ, Masutani C, Iwai S, Hanaoka F, Kunkel TA. Preferential cis-syn thymine dimer bypass by DNA polymerase eta occurs with biased fidelity. Nature. 2004; 428:97–100. [PubMed: 14999287]

(36). Johnson RE, Washington MT, Prakash S, Prakash L. Fidelity of human DNA polymerase eta. J. Biol. Chem. 2000; 275:7447–7450. [PubMed: 10713043]

(37). Bauer J, Xing G, Yagi H, Sayer JM, Jerina DM, Ling H. A structural gap in Dpo4 supports mutagenic bypass of a major benzo[a]pyrene dG adduct in DNA through template misalignment. Proc. Natl. Acad. Sci. U. S. A. 2007; 104:14905–14910. [PubMed: 17848527]

(38). Schorr S, Schneider S, Lammens K, Hopfner KP, Carell T. Mechanism of replication blocking and bypass of Y-family polymerase {eta} by bulky acetylaminofluorene DNA adducts. Proc. Natl. Acad. Sci. U. S. A. 2010; 107:20720–20725. [PubMed: 21076032]

(39). Washington MT, Johnson RE, Prakash L, Prakash S. Human DNA polymerase iota utilizes different nucleotide incorporation mechanisms dependent upon the template base. Mol. Cell Biol. 2004; 24:936–943. [PubMed: 14701763]

(40). Carlson KD, Johnson RE, Prakash L, Prakash S, Washington MT. Human DNA polymerase kappa forms nonproductive complexes with matched primer termini but not with mismatched primer termini. Proc. Natl. Acad. Sci. U. S. A. 2006; 103:15776–15781. [PubMed: 17043239]

(41). Lone S, Townson SA, Uljon SN, Johnson RE, Brahma A, Nair DT, Prakash S, Prakash L, Aggarwal AK. Human DNA polymerase kappa encircles DNA: implications for mismatch extension and lesion bypass. Mol. Cell. 2007; 25:601–614. [PubMed: 17317631]

(42). Fiala KA, Hypes CD, Suo Z. Mechanism of abasic lesion bypass catalyzed by a Y-family DNA polymerase. J. Biol. Chem. 2007; 282:8188–8198. [PubMed: 17210571]

(43). Suo Z, Johnson KA. Effect of RNA secondary structure on the kinetics of DNA synthesis catalyzed by HIV-1 reverse transcriptase. Biochemistry. 1997; 36:12459–12467. [PubMed: 9376350]

(44). Suo Z, Lippard SJ, Johnson KA. Single d(GpG)/cis-diammineplatinum(II) adduct-induced inhibition of DNA polymerization. Biochemistry. 1999; 38:715–726. [PubMed: 9888812]

(45). Suo Z, Johnson KA. DNA secondary structure effects on DNA synthesis catalyzed by HIV-1 reverse transcriptase. J. Biol. Chem. 1998; 273:27259–27267. [PubMed: 9765249]

(46). Boudsocq F, Iwai S, Hanaoka F, Woodgate R. Sulfolobus solfataricus P2 DNA polymerase IV (Dpo4): an archaeal DinB-like DNA polymerase with lesion-bypass properties akin to eukaryotic poleta. Nucleic Acids Res. 2001; 29:4607–4616. [PubMed: 11713310]

(47). Choi JY, Guengerich FP. Adduct size limits efficient and error-free bypass across bulky N2-guanine DNA lesions by human DNA polymerase eta. J. Mol. Biol. 2005; 352:72–90. [PubMed: 16061253]

(48). Gu Z, Gorin A, Krishnasamy R, Hingerty BE, Basu AK, Broyde S, Patel DJ. Solution structure of the N-(deoxyguanosin-8-yl)-1-aminopyrene ([AP]dG) adduct opposite dA in a DNA duplex. Biochemistry. 1999; 38:10843–10854. [PubMed: 10451381]

(49). Silvers KJ, Eddy EP, McCoy EC, Rosenkranz HS, Howard PC. Pathways for the mutagenesis of 1-nitropyrene and dinitropyrenes in the human hepatoma cell line HepG2. Environ. Health Perspect. 1994; 102(Suppl 6):195–200. [PubMed: 7889847]

(50). Watt DL, Utzat CD, Hilario P, Basu AK. Mutagenicity of the 1-nitropyrene-DNA adduct N-(deoxyguanosin-8-yl)-1-aminopyrene in mammalian cells. Chem. Res. Toxicol. 2007; 20:1658–1664. [PubMed: 17907783]

(51). Bacolod MD, Basu AK. Mutagenicity of a single 1-nitropyrene-DNA adduct N-(deoxyguanosin-8-yl)-1-aminopyrene in Escherichia coli located in a GGC sequence. Mutagenesis. 2001; 16:461–465. [PubMed: 11682635]

(52). Bacolod MD, Krishnasamy R, Basu AK. Mutagenicity of the 1-nitropyrene-DNA adduct N-(deoxyguanosin-8-yl)-1-aminopyrene in Escherichia coli located in a nonrepetitive CGC sequence. Chem. Res. Toxicol. 2000; 13:523–528. [PubMed: 10858326]

(53). Hilario P, Yan S, Hingerty BE, Broyde S, Basu AK. Comparative mutagenesis of the C8-guanine adducts of 1-nitropyrene and 1,6- and 1,8-dinitropyrene in a CpG repeat sequence. A slipped frameshift intermediate model for dinucleotide deletion. J. Biol. Chem. 2002; 277:45068–45074. [PubMed: 12239219]

(54). Malia SA, Basu AK. Mutagenic specificity of reductively activated 1-nitropyrene in Escherichia coli. Biochemistry. 1995; 34:96–104. [PubMed: 7819229]

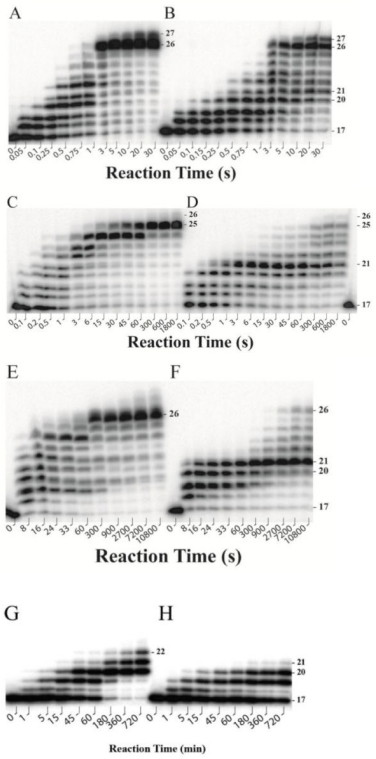

Figure 1.

Running start assays at 37 °C. A preincubated solution of 100 nM 5′-[^{32}P]-labeled 17-mer/26-mer (A, C, E and G) or 17-mer/26-mer-dG^{AP} (B, D, F and H) and 1 μM hPolη (A and B), hPolκ (C and D), hPolτ (E and F), or hRev1 (G and H) was rapidly mixed with a solution of four dNTPs (200 μM each) for various times before being quenched with 0.37 M EDTA. Sizes of important products are denoted and the 21st position marks the location of dG^{AP} from the 3′-terminus of the DNA template.

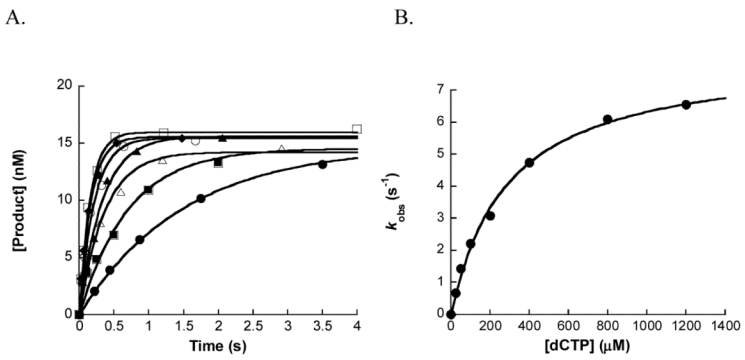

Figure 2.

Kinetics of correct dCTP incorporation onto 20-mer/26-mer-dG^{AP} catalyzed by hPolη under single-turnover conditions. (A) A preincubated solution of hPolη (130 nM) and 5′-[^{32}P]-labeled 20-mer/26-mer-dG^{AP} (20 nM) was rapidly mixed with increasing concentrations of dCTP (25 μM, •; 50 μM, ■; 100 μM, △; 200 μM, ▲; 400 μM, ○; 800 μM, ◆; 1200 μM, □) for various time intervals at 37 °C. Each time course was fit to Equation 4 to obtain a k_{obs} for a specific dCTP concentration. (B) The plot of k_{obs} values against dCTP concentrations was fit to Equation 5 to yield a $K_{d,\,dCTP}$ of 287 ± 24 μM and a k_p of 8.1 ± 0.2 s^{-1}.

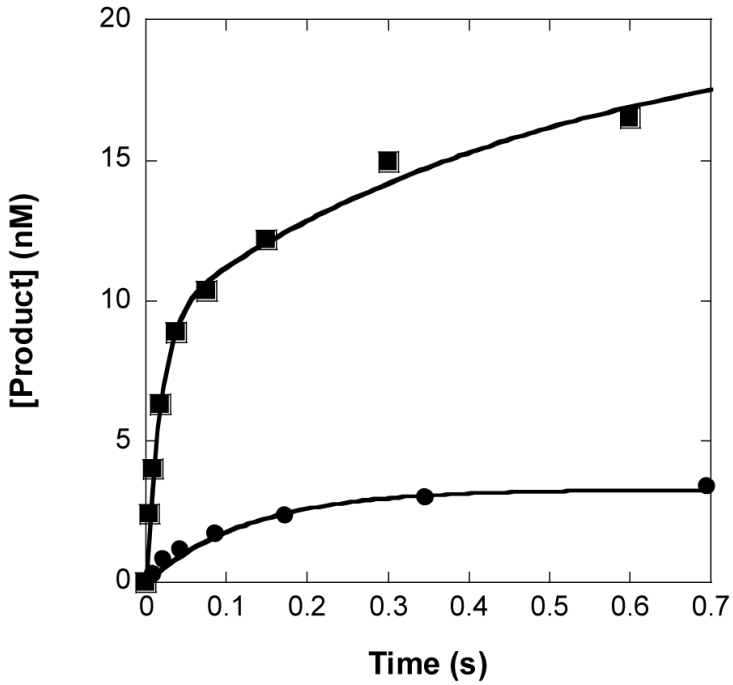

Figure 3.

Biphasic kinetics of correct dGTP incorporation onto 21-mer/26-mers catalyzed by hPolη in the presence of a DNA trap. A preincubated solution of hPolη (130 nM) and 5′-[^{32}P]-labeled 21-mer/26-mer (20 nM, ■) or 21-mer/26-mer-dG^{AP} (20 nM, •) was mixed with the solution of dGTP (0.8 mM, ■; 1.2 mM, •) and a DNA trap D-1 21/41-mer (5 μM, Table 1) for various time intervals. The plot of the product concentrations against reaction times was fit to Equation 7. For 21-mer/26-mer, the fast phase had a reaction amplitude of 7.8 ± 0.3 nM and a reaction rate constant of 72 ± 5 s^{-1} while the slow phase had a reaction amplitude of 9.5 ± 0.3 nM and a reaction rate constant of 4.4 ± 0.5 s^{-1}. For 21-mer/26-mer-dG^{AP}, the fast phase had a reaction amplitude of 2.9 ± 0.1 nM and a reaction rate constant of 11 ± 1 s^{-1} while the slow phase had a reaction amplitude of 1.1 ± 0.2 nM and a reaction rate constant of 0.20 ± 0.02 s^{-1}.

A.

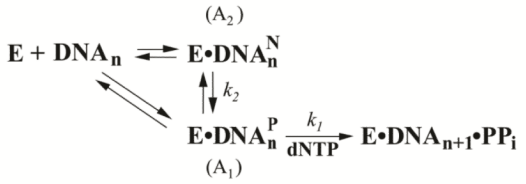

B.

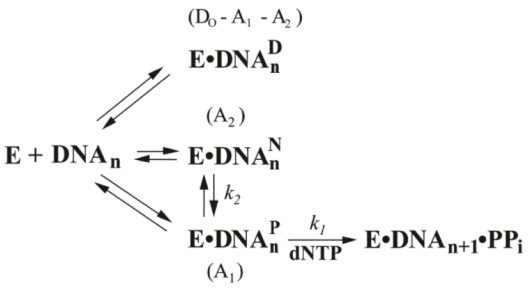

Figure 4.

Proposed kinetic mechanisms for nucleotide incorporation opposite undamaged dG (A) and damaged dG^{AP} (B) catalyzed by hPolη. A_1, fast phase amplitude; k_1, fast phase reaction rate constant; A_2, slow phase amplitude; D_o, the initial concentration of DNA; k_2, slow phase reaction rate constant; *E*, DNA polymerase; DNA_n, DNA substrate; $E•DNA^D_n$, dead-end binary complex; $E•DNA^N_n$, nonproductive binary complex; $E•DNA^P_n$, productive binary complex; $E•DNA^N_n•dNTP$, nonproductive ternary complex; $E•DNA^P_n•dNTP$, productive ternary complex; DNA_{n+1}, extended DNA product by a base; PP_i, pyrophosphate.

Table 1

DNA Substrates for dG^{AP}.

Primers	
17-mer	5′-AACGACGGCCAGTGAAT-3′
20-mer	5′-AACGACGGCCAGTGAATTCG-3′
21-mer	5′-AACGACGGCCAGTGAATTCGC-3′
Templates	
26-mer	3′-TTGCTGCCGGTCACTTAAGCGCGCCC-5′
[a] $_{26\text{-mer-}dG^{AP}}$	3′-TTGCTGCCGGTCACTTAAGCGCGCCC-5′
DNA Trap	
D-1 (21/41-mer)	5′-CGCAGCCGTCCAACCAACTCA-3′
	3′-GCGTCGGCAGGTTGGTTGAGTAGCAGCTAGGTTACGGCAGG-5′

[a] **G** designates the 1-AP adduct on C8 position of dG (dG^{AP}).

Table 2

dG^{AP} bypass efficiencies of human Y-family DNA polymerases.

Enzyme	t_{50}^{bypass} (s)[a]	t_{50} (s)[b]	t_{50}^{bypass}/t_{50}
hPolη	2.5	0.8	3.1
hPolκ	4.1	1.5	2.7
hPolτ	107	15	7.1

[a] Calculated as the time required to bypass 50% of the dG^{AP} sites.

[b] Calculated as the time required to bypass 50% of dG, or 20-mer.

Table 3

Binding affinity of hPolη, hPolτ, and hRev1 to normal and damaged DNA at room temperature.

Enzyme	DNA Substrate	With Adduct[a] (nM)	Without Adduct[b] (nM)	Affinity Ratio[c]
hPolη	20-mer/26-mer	7.9 ± 0.3	23 ± 2	3.0
	21-mer/26-mer	8.8 ± 0.5	26 ± 1	2.9
hPolτ[d]	20-mer/26-mer	64 ± 8	56 ± 12	0.9
	21-mer/26-mer	ND	43 ± 4	ND
hRev1	20-mer/26-mer	85 ± 5	118 ± 7	1.4
	21-mer/26-mer	ND	ND	ND

ND denoted ‘not determined’.

All given errors were derived from data fitting.

[a] With adduct refers to 26-mer-dG^{AP}.

[b] Without adduct refers to 26-mer.

[c] Calculated as $(K_d, \text{DNA})_{\text{Normal}}/(K_d, \text{DNA})_{\text{Damaged}}$.

[d] Values were determined using active site titration assays.

Table 4

Kinetic parameters of nucleotide incorporation onto damaged DNA catalyzed by hPolη.

dNTP	$K_{d,\ dNTP}$ (μM)	k_p (s^{-1})	$k_p/K_{d,\ dNTP}$ ($\mu M^{-1}s^{-1}$)	Efficiency Ratio[a,b]	Fidelity[c]	Fidelity Ratio[b,d]	Probability[e] (%)
Template dG^{AP} (20/26mer-dG^{AP})							
dCTP	287 ± 24	8.1 ± 0.2	2.8×10^{-2}	20	-	-	77
dATP	634 ± 66	$(8.7 \pm 0.4)\times10^{-1}$	1.4×10^{-3}	1.9	4.8×10^{-2}	10	3.9
dGTP	65 ± 7	$(5.2 \pm 0.2)\times10^{-2}$	8.1×10^{-4}	1.4	2.8×10^{-2}	14	2.2
dTTP	492 ± 67	3.0 ± 0.2	6.0×10^{-3}	1.1	1.8×10^{-1}	15	17
Template dC (21/26mer-dG^{AP})							
dGTP	125 ± 18	2.2 ± 0.1	1.8×10^{-2}	48	-	-	22
dATP	335 ± 34	$(3.3 \pm 0.1)\times10^{-1}$	1.0×10^{-3}	14	5.3×10^{-2}	3.1	1.2
dCTP	119 ± 14	7.3 ± 0.2	6.1×10^{-2}	0.3	7.7×10^{-1}	37	75
dTTP	632 ± 71	$(9.5 \pm 0.5)\times10^{-1}$	1.5×10^{-3}	3.1	7.7×10^{-2}	14	1.8

All given errors were derived from data fitting.

[a] Calculated as $(k_p/K_d, \text{dNTP})_{\text{normal}}/(k_p/K_d, \text{dNTP})_{\text{damaged}}$.

[b] The values are from Supplementary Table 1 using control 26mer DNA template.

[c] Calculated as $(k_p/K_d, \text{dNTP})_{\text{incorrect}}/[(k_p/K_d, \text{dNTP})_{\text{correct}} + (k_p/K_d, \text{dNTP})_{\text{incorrect}}]$.

[d] Calculated as $\text{Fidelity}_{\text{damaged}}/\text{Fidelity}_{\text{normal}}$.

[e] Calculated as $((k_p/K_d, \text{dNTP})_{\text{damaged}}/[\Sigma(k_p/K_d, \text{dNTP})_{\text{damaged}}])\times100$.

Chem Res Toxicol. Author manuscript; available in PMC 2013 March 19.

Table 5

Kinetic parameters of nucleotide incorporation onto damaged DNA catalyzed by hPolκ.

dNTP	$K_{d,\ dNTP}$ (μM)	k_p (s^{-1})	$k_p/K_{d,\ dNTP}$ ($\mu M^{-1}s^{-1}$)	Efficiency Ratio[a,b]	Fidelity[c]	Fidelity Ratio[b,d]	Probability[e] (%)
Template dG^{AP} (20-mer/26-mer-dG^{AP})							
dCTP	267 ± 40	1.7 ± 0.1	6.5×10^{-3}	5.7	-	-	71
dATP	497 ± 98	$(7.0 \pm 0.6)\times10^{-1}$	1.4×10^{-3}	0.4	1.8×10^{-1}	11	15
dGTP	346 ± 80	$(3.4 \pm 0.3)\times10^{-1}$	9.9×10^{-4}	1.1	1.3×10^{-1}	4.5	11
dTTP	726 ± 237	$(2.4 \pm 0.4)\times10^{-1}$	3.2×10^{-4}	2.5	4.7×10^{-2}	2.2	3.5
Template dC – pause site (21-mer/26-mer-dG^{AP})							
dGTP	43 ± 7	$(2.3 \pm 0.1)\times10^{-3}$	5.3×10^{-5}	208	-	-	60
dATP	203 ± 36	$(5.5 \pm 0.3)\times10^{-3}$	2.7×10^{-5}	1.5	3.4×10^{-1}	94	31
dCTP	693 ± 45	$(4.1 \pm 0.1)\times10^{-3}$	5.9×10^{-6}	12	1.0×10^{-1}	17	6.7
dTTP	468 ± 90	$(12 \pm 1)\times10^{-4}$	2.5×10^{-6}	16	4.5×10^{-2}	13	2.8

All given errors were derived from data fitting.

[a] Calculated as $(k_p/K_d, \text{dNTP})_{\text{normal}}/(k_p/K_d, \text{dNTP})_{\text{damaged}}$.

[b] The values are from Supplementary Table 2 using control 26mer DNA template.

[c] Calculated as $(k_p/K_d, \text{dNTP})_{\text{incorrect}}/[(k_p/K_d, \text{dNTP})_{\text{correct}} + (k_p/K_d, \text{dNTP})_{\text{incorrect}}]$.

[d] Calculated as $\text{Fidelity}_{\text{damaged}}/\text{Fidelity}_{\text{normal}}$.

[e] Calculated as $((k_p/K_d, \text{dNTP})_{\text{damaged}}/[\Sigma(k_p/K_d, \text{dNTP})_{\text{damaged}}])\times100$.

Table 6

Kinetic parameters of nucleotide incorporation onto damaged DNA catalyzed by hPolτ.

dNTP	K_d, dNTP (μM)	k_p (s^{-1})	k_p/K_d, dNTP ($\mu M^{-1}s^{-1}$)	Efficiency Ratio[a,b]	Fidelity[c]	Fidelity Ratio[b,d]	Probability[e] (%)
Template dG^{AP} (20-mer/26-mer-dG^{AP})							
dCTP	380 ± 66	$(8.8 \pm 0.6)\times10^{-2}$	2.3×10^{-4}	7.0	-	-	97
dATP	338 ± 22	$(10.3 \pm 0.2)\times10^{-4}$	3.0×10^{-6}	5.0	1.3×10^{-2}	1.4	1.3
dGTP	252 ± 29	$(5.3 \pm 0.2)\times10^{-4}$	2.1×10^{-6}	7.6	9.0×10^{-3}	0.9	0.9
dTTP	762 ± 60	$(13.1 \pm 0.5)\times10^{-4}$	1.7×10^{-6}	118	7.3×10^{-3}	0.1	0.7
Template dC – pause site (21-mer/26-mer-dG^{AP})							
dGTP	264 ± 76	$(5.9 \pm 0.6)\times10^{-5}$	2.2×10^{-7}	4.5×10^{3}	-	-	47
dATP	ND	ND	-	-	-	-	-
dCTP	ND	ND	-	-	-	-	-
dTTP	573 ± 73	$(14.1 \pm 0.8)\times10^{-5}$	2.5×10^{-7}	680	5.3×10^{-1}	5.5	53

ND denoted ‘not determined’.

All given errors were derived from data fitting.

[a] Calculated as $(k_p/K_d, \text{dNTP})_{\text{normal}}/(k_p/K_d, \text{dNTP})_{\text{damaged}}$.

[b] The values are from Supplementary Table 3 using control 26mer DNA template.

[c] Calculated as $(k_p/K_d, \text{dNTP})_{\text{incorrect}}/[(k_p/K_d, \text{dNTP})_{\text{correct}} + (k_p/K_d, \text{dNTP})_{\text{incorrect}}]$.

[d] Calculated as $\text{Fidelity}_{\text{damaged}}/\text{Fidelity}_{\text{normal}}$.

[e] Calculated as $((k_p/K_d, \text{dNTP})_{\text{damaged}}/[\Sigma(k_p/K_d, \text{dNTP})_{\text{damaged}}])\times100$.

Chem Res Toxicol. Author manuscript; available in PMC 2013 March 19.

Table 7

Kinetic parameters of nucleotide incorporation onto damaged DNA catalyzed by hRev1.

dNTP	$K_{d,\ dNTP}$ (μM)	k_p (s^{-1})	$k_p/K_{d,\ dNTP}$ ($\mu M^{-1}s^{-1}$)	Efficiency Ratio[a,b]	Fidelity[c]	Fideltiy Ratio[c]	Probability[e] (%)
Template dG^{AP} (20-mer/26-mer-dG^{AP})							
dCTP	5.2 ± 0.9	$(3.3 \pm 0.2)\times10^{-2}$	6.5×10^{-3}	22	-	-	99.8
dTTP	78 ± 18	$(2.6 \pm 0.3\times10^{-4}$	3.4×10^{-6}	7.6×10^{3}	5.2×10^{-4}	3.0×10^{-3}	0.1
dATP	103 ± 25	$(4.4 \pm 0.4\times10^{-4}$	4.2×10^{-6}	17	6.5×10^{-4}1.3	1.3	0.1
dGTP	143 ± 34	$(4.2 \pm 0.3)\times10^{-4}$	3.0×10^{-6}	1.8×10^{3}	4.6×10^{-4}	0.1	~0

All given errors were derived from data fitting.

[a] Calculated as $(k_p/K_d, \text{dNTP})_{\text{normal}}/(k_p/K_d, \text{dNTP})_{\text{damaged}}$.

[b] The values are from Supplementary Table 4 using control 26mer DNA template.

[c] Calculated as $(k_p/K_d, \text{dNTP})_{\text{incorrect}}/[(k_p/K_d, \text{dNTP})_{\text{correct}} + (k_p/K_d, \text{dNTP})_{\text{incorrect}}]$.

[d] Calculated as $\text{Fidelity}_{\text{damaged}}/\text{Fidelity}_{\text{normal}}$.

[e] Calculated as $((k_p/K_d, \text{dNTP})_{\text{damaged}}/[\Sigma(k_p/K_d, \text{dNTP})_{\text{damaged}}])\times100$.

Chem Res Toxicol. Author manuscript; available in PMC 2013 March 19.